A ResUNet Model for NDVI-based Deforestation Prediction in Galicia, Spain: Combining Spectral and Ontological Data

Christy Esmee Mulder[1]

Vrije Universiteit,
Amsterdam, The Netherlands
cmu201@student.vu.nl
Supervisor: M. Cochez
m.cochez@vu.nl

Abstract. Deforestation poses a significant risk to global ecosystems, especially in fire-prone locations such as Galicia, Spain. This research presents an approach to predicting the changes in vegetation health by incorporating detailed ontological data and spectral data from Sentinel-2A imagery using the modified ResUNet-O model. The Normalized Difference Vegetation Index (NDVI) is used as a primary measure to assess the vegetation health, combined with functional traits of trees such as tree species, height, and volume of firewood obtained from the Cross-Forest ontology. The methodology uses satellite imagery from 2017-2018 and advanced deep learning techniques to improve the accuracy of predictions made by the hybrid ResUNet architecture. An ablation study demonstrates that the ResUNet architectures outperform conventional deep learning models such as ResNet-18 and CNN architectures. The ResUNet-O model shows enhanced performance when ontological data is present, in contrast to its absence. Although the research shows promising results, it also acknowledges limits in the incompleteness of the data and the temporal resolution. Despite the promising results, the research acknowledges limitations in data incompleteness and temporal resolution, suggesting new fields for future work in feature evaluation and dataset augmentation. This research ultimately contributes to the advancement of forest monitoring techniques, offering a robust tool for environmental management and conservation efforts in wildfire-prone regions like Galicia, Spain.

Keywords: Deforestation · Ontology · Sentinel-2A · ResU-Net · NDVI · Galicia · Computer Vision · Forest Monitoring · Deep Learning

1 Introduction

Forests have a crucial role in preserving ecological balance, promoting biodiversity, and reducing the impacts of climate change. Nevertheless, they are progressively challenged by the process of deforestation and a variety of environmental stressors. Land use and land cover change (LULCC), particularly deforestation caused by wildfires, is a major factor contributing to this threat. It has enormous effects on ecosystems and the dynamics of climate, as mentioned in the study by [23]. Research suggests a significant correlation between deforestation caused by wildfires and the degradation of the ecosystem. This is further accelerated by global warming, climate change [23], and human activities such as population increase and economic development [13].

Spain, particularly the Galicia region, has a long history of being severely affected by wildfires [3]. The forests in Galicia have suffered extensive destruction, primarily affecting maritime pine, various oak species, and eucalyptus trees. Between 1961 and 2011, the region encountered a total of 245,593 wildfires, resulting in the destruction of 1,794,578 hectares of land. This accounts for almost 62% of the region's overall geographical area and nearly 87% of its entire forested area [9]. The wildfires are influenced by both socioeconomic and meteorological elements, which highlights their complex dynamics of deforestation and the importance of implementing prevention programs that are tailored to the individual location [7].

To effectively reduce deforestation, it is important to employ advanced monitoring techniques to establish accurate and diverse datasets. In order to tackle these difficulties, the Cross-Forest Project, led by Gimenez-Garcia [12], created an ontology that combines information from forest inventories and land cover maps of The Iberian Peninsula. This ontology offers detailed information about monitored trees, including their species [12], providing valuable features for the purpose of this research.

Advancements in deep learning techniques and remote sensing data have recently enhanced the accuracy and monitoring of deforestation in particularly vulnerable regions, such as the Amazon forests [5]. Deep learning and other machine learning algorithms are currently used to forecast deforestation [1], [31], despite the complex dynamics of the problem caused by interactions within human-ecological systems.

A major limitation of existing deforestation prediction models that utilize satellite images is their inability to consider the vulnerability of different tree species, and other functional traits, to fire. Research suggests that certain tree species have a higher susceptibility to forest fires compared to others [26]. Failure to include this essential aspect in models might result in underestimating or misrepresenting the risk of fire-induced deforestation, which in turn may undermine the effectiveness of forest management policies. While satellite imagery, such as from Sentinel-2A, provides valuable data for monitoring forest conditions, it is often insufficient on its own to fully capture the complexities of forest ecosystems. In order to enhance the accuracy of forest health forecasts, it is crucial to incorporate additional, diverse and comprehensive data, including, but not limited to:

- *Data on Tree Species:* Tree species have diverse fire susceptibilities, growth rates, and ecological functions[25], [26]. Integrating ontological data with tree species might enhance the predictive capabilities of models in identifying

regions that are more susceptible to deforestation caused by wildfires or other contributing factors [11].
- Volume of firewood: An analysis of the firewood volume in various forest zones can offer valuable information about the probable severity and extent of wildfires. Regions with greater firewood quantities are more susceptible to intense wildfires, which can profoundly impact deforestation trends [25], [26].
- *Tree Height:* Comprehensive data regarding the height of trees and the layout of forests can improve our comprehension of the dynamics and well-being of forest ecosystems [16]. Taller trees or dense forest canopies may display distinct fire behavior and resistance in comparison to shorter or less dense flora [14].

Despite extensive research on the effects of Land Use and Land Cover Change (LULCC), there is still a critical need for more precise and comprehensive models to forecast the health of forests. Current approaches frequently fail to incorporate diverse data sources, which restricts their ability to fully capture the complex dynamics of forest ecosystems and the various dimensions of deforestation effects. Existing methods have limitations, which is why a mixed approach is proposed. The approach in this research combines U-Net and ResNet models and uses datasets such as multitemporal imagery from satellites and ontological data layers to forecast vegetation health values for every pixel in the image.

This approach employs a the backbone of a U-Net [21], which is specifically designed to identify changes in the health of vegetation, particularly the Normalized Difference Vegetation Index (NDVI) [17]. It is combined with a pre-trained ResNet-18 model; the result is a ResUNet architecture. The specific objectives of this research are:

1. To integrate ontological data with remote sensing data to improve NDVI predictions.
2. To detect regions in Galicia that are more susceptible to deforestation.

The method uses high-resolution Sentinel-2A satellite images from the years 2017-2018. It also incorporates specific data on tree species, firewood volume, and tree height, which are retrieved from the Cross-Forest ontology. The RGB, NIR, and NDVI bands of the Sentinel-2A satellite images serve as a reference for forecasting the NDVI in subsequent years. In addition, three additional ontological bands are generated using the Cross-Forest features and combined with the existing satellite bands to offer context-specific data that influences vegetation health and dynamics. An ablation study is conducted to compare the performance of the ResUNet model with other models such as CNN and ResNet.

The results show that by incorporating ontological layers, the predicted accuracy of NDVI is enhanced. This methodology enables the model to consider the details of the functional tree traits, which result in more accurate forecasts for forest monitoring. Ultimately, this research aims to enhance the accuracy of predicting changes in forest vegetation health in Galicia, Spain by combining satellite imagery with ontological data.

The remaining part of this paper is organized as follows: Section 2 reviews related work on including functional traits, deep neural networks and remote sensing in forest monitoring and the NDVI. Section 3 discusses the methodology in detail, presenting the proposed ResUNet-O model and the ontological feature layers. Section 4 provides an ablation study and analysis of the results, including model performance. Section 5 discusses the ablation study, model performance and limitations. Finally, Section 6 concludes the paper with a summary of findings, contributions of this paper and implications for future research.

2 Related Work

2.1 Functional Traits for Prediction of Complex Dynamics

In order to improve model learning and capture the complex correlations between tree traits, studies have been looking into ways to incorporate extra variables. [10] created generalized mixed-effects height–DBH (Diameter at Breast-Height) models for mixed forests in Northeastern China. These models incorporated species functional features, including leaf economic spectrum features, maximum tree height, and wood density, into the base model. The functional features had a substantial impact, resulting in improved estimations between relationships and an increase in the accuracy of carbon stock assessment by 82.42% [10]. Similarly, by combining data from canopy height maps and tree species classifications, regression models for predicting timber volume have been proved to show a higher accuracy. This approach is especially efficient in forest environments with diverse structures, as it allows for the combination of different data sources to reduce misclassification effects and enhance the reliability of the model [14].

For accessing a variety of forestry data, the usage of ontologies such as the cross-forest ontology is essential. The Cross-Forest project [12] shows the use of ontologies to establish standardization and establish connections across forest inventory data, hence enhancing its accessibility and compatibility for diverse applications. Recent research emphasizes the significance of diverse datasets and advanced modeling techniques. For instance, by incorporating several variables, such as environmental and management features, greatly improves prediction accuracy in a machine-learning-based strategy for forecasting deforestation associated with oil palm plantations [24].

In addition, advanced modeling techniques, like those used by the *forestatrisk* Python package, demonstrate that accurately predicting deforestation requires the integration of multiple spatial explanatory factors. These factors include terrain, accessibility, deforestation history, and land conservation status. Previous research has shown that incorporating these factors into models greatly enhances the ability to accurately anticipate deforestation patterns and offers essential insights for decision and policy makers [22], [11]. An example of this is a study that used a model to analyze deforestation in the southern Yucatán peninsular region. The study found that using various spatial factors was successful in predicting changes in land use. This supports the comprehensive approach taken by *forestatrisk* [11]. These methods emphasize once again the significance of incorporating a variety of data sources to accurately capture the complex dynamics of deforestation.

2.2 Deep Neural Networks and Remote Sensing in Forest Monitoring

Advanced monitoring techniques, such as the use of remote sensing data and the deployment of deep learning models, have shown promising capabilities in predicting and monitoring deforestation. These methods make it possible to detect regions of vulnerability and carry out targeted interventions to decrease future environmental damage [31].

Recent research has shown that incorporating several spatial and temporal variables might enhance the accuracy of deforestation predictions. An example of this is a research by [2] that utilized, among others, deep convolutional neural networks (CNNs) to analyze multispectral satellite data, annual forest change maps, and digital surface models. The purpose of this research was to accurately predict deforestation patterns. The models successfully detected deforestation risks by examining various factors, including both natural and human-induced factors, such as the distance to highways and historical deforestation data [2]. Other models tested in this research entail hybrid machine learning models, which merge dense neural networks with long-short term memory (LSTM) networks. They have demonstrated potential in forecasting deforestation by integrating multiple datasets, such as geographical, meteorological, and socio-economic features [2].

The incorporation of remote sensing data with sophisticated machine learning models, such as semantic segmentation and deep learning, shows great potential for enhancing forest monitoring. These algorithms can utilize high-resolution satellite images to identify and categorize alterations in forest cover with enhanced accuracy. Nevertheless, according to [1], further research is required to examine the efficacy of these models in monitoring deforestation.

Furthermore, the architecture of a ResUNet model integrates features of a U-Net and a ResNet, making it highly suitable for semantic segmentation tasks in remote sensing applications. The incorporation of residual connections improves the model's capacity to handle spatial patterns and maintain high accuracy across different scales, demonstrating its significant efficacy for deforestation monitoring tasks[6].

The high resolution satellite images, used by for instance, [4] that employed Landsat imagery to monitor deforestation and forest degradation on a worldwide scale. They emphasize the significance of satellite data in comprehending forest dynamics. While several studies utilize Landsat data with a spatial resolution of 30 meters, Sentinel-2A satellite imagery provides a more refined spatial resolution of 10 meters, with the NIR band having a resolution of 20 meters. Research conducted using Sentinel-2A data in Google Earth Engine has demonstrated that its high-resolution, multispectral imagery is highly suitable for remote sensing applications, such as deforestation monitoring [19]. This provides the preference for the usage of Sentinel-2A satellite imagery in this research over Landsat satellite imagery.

2.3 NDVI

The Normalized Difference plants Index (NDVI) is a commonly used metric in remote sensing that is used to evaluate vegetation heatlh. The Normalized Difference Vegetation Index (NDVI) is calculated, as depicted in the formula below, by subtracting the red band value (RED) from the near-infrared band value (NIR), and then dividing the result by the sum of the NIR and RED values.

$$\mathrm{NDVI} = \frac{\mathrm{NIR} - \mathrm{RED}}{\mathrm{NIR} + \mathrm{RED}}$$

NDVI values range between -1 and 1. Vegetation that is in good health reflects near-infrared (NIR) light and absorbs red light, which leads to higher values of the Normalized Difference Vegetation Index (NDVI). On the other hand, barren fields, lake bodies, and urban areas have lower NDVI values. The index presented here offers a quantitative assessment of the density and state of vegetation [28], making it an essential measure for monitoring the vegetation health of forests and identifying deforestation.

The NDVI is generally used as the target label in various research due to its efficacy in accurately representing the condition of vegetation [20]. It acts as a substitute for other characteristics of plants, such as the amount of canopy coverage, and the general condition of the plant. Moreover, the calculation of NDVI using satellite data is rather straightforward, and this data is accessible in several spatial and temporal resolutions, making it convenient for extensive forest monitoring.

Many studies have used the NDVI to monitor the state of forests and make predictions about deforestation [30], [8]. For example, [30] used the NDVI to monitor changes in vegetation in China due to climate change and human activities. Their study showed the effectiveness of the NDVI in monitoring ecological changes on a wider scale. Similarly, [8] used the NDVI to observe changes in vegetation in the Sahel region. They emphasized that NDVI is responsive to both changes in climate and human activities. The incorporation of NDVI with machine learning techniques has increased its usage in deforestation research. As previously stated, the article by [1] addresses the limited availability of extensive datasets for forests in Jordan. It highlights the significance of using NDVI as a key variable in machine learning models that aim to monitor deforestation through satellite imaging. Nevertheless, existing machine learning techniques frequently come across difficulties in effectively capturing local contexts, as highlighted by [2]. They also mention the necessity for conducting more localized research and developing semantic segmentation models to enhance deforestation monitoring.

3 Methodology

In this section the methodology of this study is presented, including the proposed ResUNet-O model, the procedure for collection and preparation of the datasets, the creation of the ontology layers, and the procedure of deforestation modeling.

3.1 Study Region

The region of interest encompasses a large part of Galicia. The specific area studied covers 26,042 km^2, defined by the coordinates latitude -8.599948 to -6.711535 and longitude 41.797418 to 43.308103. Galicia, with a total surface area of 29,574 km^2, is similar in size to the regions examined in related studies, such as those by Matosak et al. [18], which used areas of approximately 35,200 km^2 and 27,500 km^2. This study area size is adequate to provide reliable deforestation predictions due to its substantial coverage and diversity of forest types.

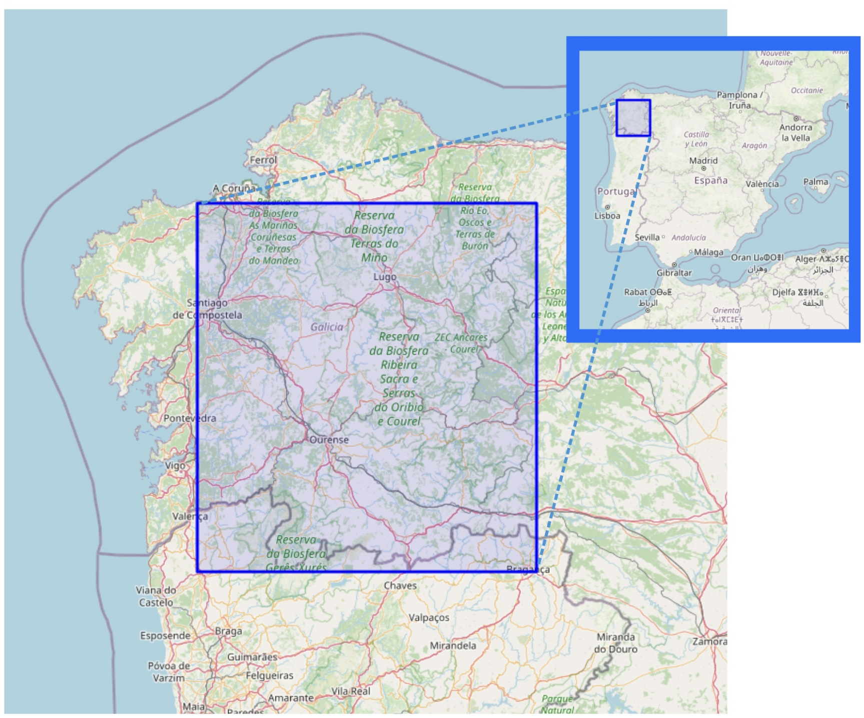

Fig. 1. Map of the study region in Galicia.

3.2 Satellite Imagery

To ensure easy replication and scalability, the dataset is limited to globally freely accessible sources. The primary data involves satellite imagery from the Sentinel 2 mission, a collaboration between the European Commission and the European Space Agency (ESA) as part of the Copernicus program. The images have a spatial resolution of 10 meters per pixel and cover an annual time series from January 2017 to June 2024, as depicted in Table 1.

Name	Scale	Pixel Size	Wavelength	Description
B2	0.0001	10 meters	496.6nm (S2A) / 492.1nm (S2B)	Blue
B3	0.0001	10 meters	560nm (S2A) / 559nm (S2B)	Green
B4	0.0001	10 meters	664.5nm (S2A) / 665nm (S2B)	Red
B8	0.0001	20 meters	703.9nm (S2A) / 703.8nm (S2B)	Red Edge 1

Table 1. Spectral Band Information of the Sentinel-2A satellite[1]

For the remote sensing data of Galicia, bands 4 (red) and 8 (near-infrared) are used to calculate the Normalized Difference Vegetation Index (NDVI), which is crucial for assessing vegetation health. The images are collected through Google Earth Engine, which combines a catalog of satellite imagery and geospatial datasets. The collected images, after processing, total 3969 images with dimensions of 256x256 pixels each.

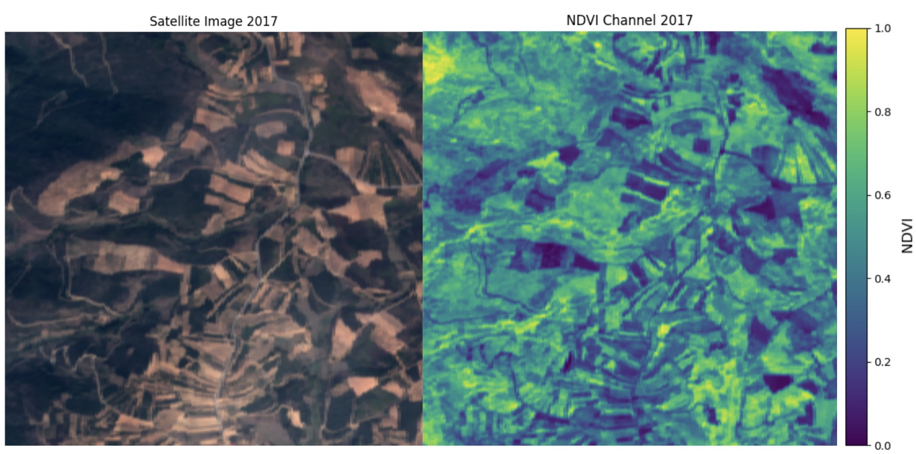

Fig. 2. Satellite images of 2017 in RGB and NDVI bands

[1] More information can be found at the Google Earth Engine Documentation.

To avoid interference from clouds, a cloud filter was set to 20%, allowing only images with less than 20% cloud cover to be used. Additionally, the area was selected to exclude water bodies to ensure that only terrestrial vegetation is analyzed.

3.3 Normalized Difference Vegetation Index

3.3.1 Data Collection and Preprocessing

After downloading the satellite data from Google Earth Engine, the images were preprocessed to ensure access to the correct bands. The selected bands for each image were RGB, NIR, and NDVI. The NDVI was calculated using Sentinel-2A imagery with a spatial resolution of 10 meters, where Band 4 (B4) represents the red band, and Band 8 (B8) represents the near-infrared (NIR) band. This calculation provides a value for each pixel indicating vegetation health, with higher values indicating healthier vegetation. Figure X shows the specifications of these bands for the Sentinel-2A satellite data.

3.3.2 Noise and Error Considerations

NDVI data can be influenced by various sources of noise, including sensor resolution, ground conditions, and atmospheric conditions. These factors can create errors and noise in the NDVI measurements, which must be accounted for in the analysis [20]. Common sources of NDVI noise include cloud coverage, snow, water, and shadows. To decrease these effects, several smoothing techniques can be used, such as:

- Best Index Slope Extraction (BISE)
- Weighted Least-Squares Linear Regression
- Maximum Value Compositing (MVC)
- Curve-Fitting
- Step-Wise Logistic Regression

These methods help prevent false high NDVI values caused by noise and ensure more reliable vegetation health assessments [20]. While most errors tend to decrease NDVI values, accurate noise reduction is crucial for obtaining dependable results.

In this research, these methods have been considered; however, due to scope limitations, manual methods were not applied. Instead, the automated cloud filtering provided by Google Earth Engine (GEE) is utilized, which effectively reduces noise from cloud coverage. To further reduce noise, the satellite data used in this research represent an average of images collected throughout the year. This averaging process reduces the impact of transient conditions such as clouds and shadows. However, to ensure the robustness of the model, images with more than 20% cloud cover were excluded from the dataset.

It is worth noting that additional experiments with different cloud filter thresholds could provide insights into the influence of cloud cover on NDVI accuracy. By training the model with various cloud filters, the impact of these conditions on NDVI predictions can be better understood. By addressing these noise and error considerations, the NDVI data used in this study were refined to provide accurate and reliable indicators of vegetation health. This preprocessing ensures that the NDVI predictions from the model are robust and effective for monitoring forest health in Galicia, Spain.

3.4 Cross-Forest Ontology

The Forest Explorer[2] is a web application developed by [12] based on the ontologies of the Cross-Forest project[3]. This project aims to make the Iberian forest inventories and land cover maps accessible to potential users. The web application provided valuable insights into tree mappings, and serves as a foundational dataset for this study.

The Cross-Forest project integrates data from four primary sources: the Spanish National Forest Inventory (IFNes), the Portuguese National Forest Inventory (IFNpt), the Spanish Forest Map (MFE), and the Portuguese Land Use Map (COS). Specifically, it includes datasets from the Third Spanish Forest Inventory (IFN3 for Spain), the Spanish Land Cover Map 1:50,000 (MFE50 for Spain), the Spanish Soil Erosion Inventory (INES for Spain), the Sixth Portuguese Forest Inventory (IFN6 for Portugal), the Portuguese Land Cover Map 2018 (COS18 for Portugal), and Iberian Forest Fires Statistics.

Province	Trees (#)	Basal area (m^2)	Volume (m^3)	Trees in inv.	Plots in inv.
La Coruna	194,617,033	5,624,608	40,804,528	42,533	2,558
Lugo	254,827,943	7,913,506	46,220,913	34,915	1,833
Pontevedra	99,880,833	3,250,974	23,435,638	19,527	1,118
Orense	135,736,144	4,083,619	22,631,675	18,398	1,325
Total Galicia	**685,061,953**	**20,872,707**	**133,092,754**	**115,373**	**6,834**

Table 2. Forest Inventory Data of Cross-Forest Ontology by Province in Galicia [12]

According to Forest Explorer, there are nearly 700 million trees in Galicia, and the National Forest Inventory (IFN3) records nearly 7 trillion trees in Spain between 1997 and 2008. Of these, the Forest Explorer includes 115,373 trees in its inventory, with 66,352 trees falling within the region of interest that contain all three features: tree species, height, and volume of firewood, depicted in Table 3. There are 70 different tree species in the region of interest.

[2] https://forestexplorer.gsic.uva.es/explorer/
[3] https://crossforest.gsic.uva.es/sparql

Species_no	Species_name	Count	Percentage
26	Pinus pinaster	22460	33.85
41	Quercus robur	10843	16.34
61	Eucalyptus globulus	7132	10.75
21	Pinus Sylvestris	5640	8.50
72	Castanea sativa	4598	6.93
43	Quercus pyrenaica	4468	6.73
28	Pinus radiata	4430	6.68
273	Betula alba	2310	3.48
54	Alnus glutinosa	938	1.41
46	Quercus suber	443	0.67
62	Eucalyptus camaldulensis	302	0.46
364	Eucalyptus Gomphocephala	291	0.44
357	Salix atrocinerea	265	0.40
73	Betula	237	0.36
65	Eucalyptus Nitens	211	0.32
Other	55 different species	2351	3.54
Total	**All species**	**66352**	**100.00**

Table 3. Species Count and Percentage Distribution

In the context of this research, the Cross-Forest ontology is used alongside satellite imagery as the primary dataset. Despite the unspecified time of registration for this data, it is assumed to be time-insensitive, which limits this research to a certain extent.

3.5 Feature Extraction and Engineering

3.5.1 Sentinel-2A

The primary features extracted from the Sentinel-2A satellite imagery include the red (B4) and near-infrared (NIR, B8) bands, which are used to calculate the NDVI. The area of interest (AOI) is a rectangular region in Galicia, covering 26,042 km^2 and ensuring only vegetated areas are included. Data extraction dates range from January 1, 2017, to December 30, 2017, focusing on the bands B4 (Red), B3 (Green), B2 (Blue), and B8 (NIR). The NDVI is calculated for each pixel by taking the normalized difference between the Red and NIR bands and stored as an additional fifth band for each image.

The image collection for the entire year is averaged into a single composite image, where the intensity values of each pixel across all images are averaged. This composite image is georeferenced, meaning each pixel has specific coordinates tied to a referencing system, facilitating accurate mapping and analysis. A 20% cloud filter is applied to ensure accurate pixel representation. The images are then sliced into seven segments, resulting in a total of 49 images with dimensions of 2400 by 2400 pixels for manageable downloads.

3.5.2 Cross-Forest Ontology

The Cross-Forest ontology provides detailed information on tree species, firewood volume, and tree height, all of which are georeferenced. Ontological data, including tree height, firewood volume, and species, is extracted from the Cross-Forest SPARQL endpoint. This data is cleaned by removing irrelevant columns, retaining only the three features and their corresponding coordinates. The trees are sorted and stored in a dictionary that contains the coordinate boundaries of the 49 satellite image tiles, ensuring each tree is correctly placed within its corresponding coordinates.

Data preprocessing involves normalizing all values to a common scale with values between 0 and 1, to ensure compatibility and enhance model performance. The normalized data is then mapped to each tile, with a radius of 50 pixels assigned to each tree to represent its area more accurately. This step accounts for the sparse tree data in the ontology by expanding the representation area, assuming that the presence of one tree suggests the likelihood of more trees of the same species in the vicinity.

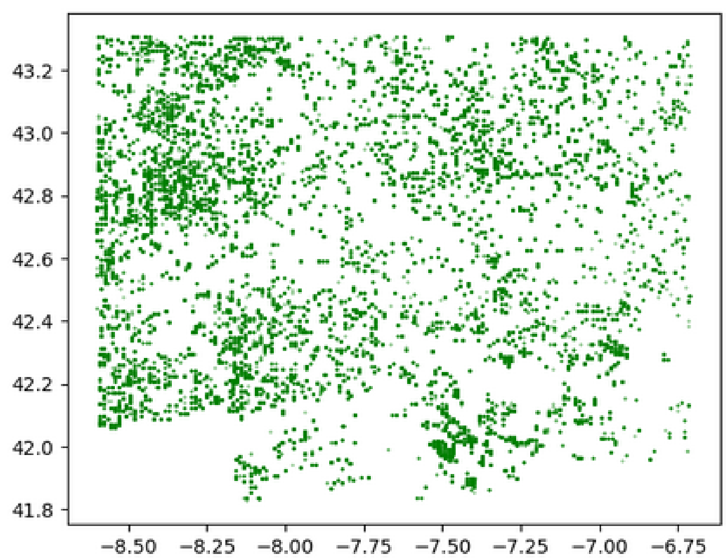

Fig. 3. A mask visualization of all trees from the ontology dataset, mapped over the area of interest. The points indicate the geographical locations of individual trees. The axes depict the coordinates.

The processed data is stored in tensors with normalized values for each feature at specific locations corresponding to the coordinates of the trees. This creates new ontology layers, with each feature (species, height, and firewood volume) having its own layer. These layers are later combined with the satellite imagery to create a composite image that includes all relevant data. Each tensor has dimensions of 256 by 256.

The ontology layers are then added to the satellite images, resulting in a dataset consisting out of 3969 images of a dimension of 256x256 with eight channels: RGB, NIR, NDVI, species, height, and firewood volume.

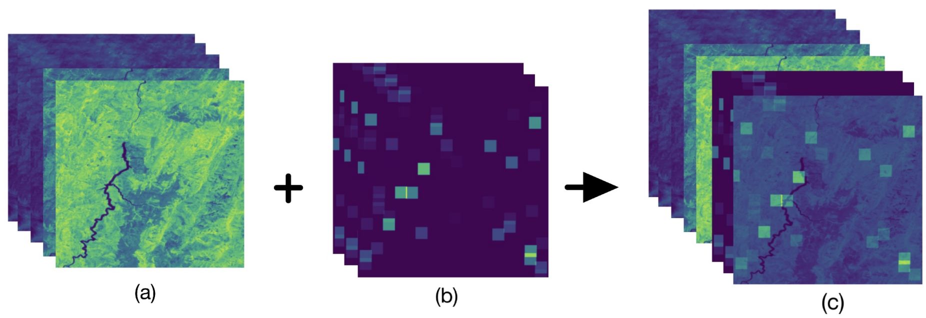

Fig. 4. (a) Five base bands of the Sentinel-2A imagery: RGB, NIR and NDVI. (b) Three generated ontological bands based on the features "species", "height", "volume of firewood". (c) A combined dataset of 8 channels; a combindation of (a) and (b)

3.6 Model Development

The approach of the creation of the ResUNet-O model differs from conventional applications of ResUNet by considering vegetation health prediction as a regression problem instead of a segmentation problem. The model predicts a normalized value, which gives a precise measure of changes in vegetation health. To be more specific, the ResUNet-O model takes Sentinel-2A data from 2017 as input, consisting of eight spectral channels, to predict the NDVI values for 2018. The model produces a single channel of NDVI for that specific year as an output. This provides a more detailed overview of regions that are at risk of deforestation. Recent research has demonstrated that uses deep learning models for regression tasks can successfully capture the intricate patterns of environmental factors, hence improving the accuracy of predictions for vegetation health measurements such as NDVI [27].

3.6.1 Model Architecture

The ResUNet-O model developed in this research is a combination of a U-Net backbone and a pre-trained ResNet architecture on top of that to leverage their both strengths. Specifically, it is designed to handle inputs with eight channels, integrating spectral and ontological data, and produce a single-channel output representing the predicted NDVI values.

The encoder of the ResUNet model is based on a modified pre-trained ResNet-18 architecture. The first convolutional layer is adapted to accept eight input channels, to include RGB, NIR, NDVI, tree species, height, and firewood volume. This layer employs a 7x7 convolution with a stride of 2 and padding of 3, followed by batch normalization and ReLU activation. The output continues through a max-pooling layer.

The decoder comprises four upsampling blocks, reversing the encoding process by increasing spatial dimensions and reducing feature depth. Each block handles skip connections from the corresponding encoder layers, preserving spatial information by concatenating with the upsampled features. Each block includes a transpose convolution layer, followed by two convolutional layers with batch normalization and ReLU activation. The upsampling blocks are detailed as follows:

- UpBlock3: Upsamples the output of the fourth encoder block (512 channels) to 256 channels and concatenates it with the third encoder block's output (256 channels).
- UpBlock2: Upsamples the output of UpBlock3 (256 channels) to 128 channels and concatenates it with the second encoder block's output (128 channels).
- UpBlock1: Upsamples the output of UpBlock2 (128 channels) to 64 channels and concatenates it with the first encoder block's output (64 channels).
- UpBlock: Upsamples the output of UpBlock1 (64 channels) to 64 channels and concatenates it with the initial output (64 channels).

After the upsampling blocks, a final upsampling layer restores the original spatial dimensions using a transpose convolution. The model ends with a single convolution layer, reducing the feature depth to the desired output channel and produces the final NDVI prediction map.

3.6.2 Data Preperation

The dataset of the 2017 satellite images, consisting of 3969 samples with a shape of (8, 256, 256), was divided into training, validation, and test sets. The dataset was divided, with 20% (794 samples) allocated for the test set, while the remaining 3175 samples were used for training and validation. A 5-fold cross-validation was used to divide the training/validation set into smaller subsets, allowing the model to be validated on diverse sets and improving its capacity to generalize. The training and validation batch size was set to 16, which guarantees computationally reasonable operations. The data preparation process uses a manually created dataloader that is responsible for loading and organizing satellite pictures together with their respective NDVI targets.

3.6.3 Training Process

The training process aimed to optimize the ResUNet-O model's performance using a Mean Squared Error (MSE) loss function, suitable for NDVI prediction tasks. The Adam optimizer was used with a learning rate of 0.001 over 10 epochs. The training steps included:

- Model Initialization: Instantiating the ResUNet-O model with 8 input channels and 1 output channel.
- Loss Function and Optimizer: Employing the MSE loss function and using the Adam optimizer with a learning rate of 0.001.
- Epochs and Iterations: Training the model for 10 epochs, each consisting of multiple iterations over the training dataset.

After each epoch, the model's performance was evaluated on the validation set to monitor its generalization ability. The model was trained and evaluated on each fold, and the performance metrics (MAE, RMSE, $\mathbf{R^2}$) were calculated to assess the model's accuracy and reliability. Additionally, the average test loss across all folds was calculated to provide an overall assessment of the model's predictive capability. The trained models for each fold were saved for future use and analysis.

3.6.4 Evalulation Metrics

To assess the performance of the models developed, several evaluation methods are used. These metrics provide a valuable insight into the accuracy, reliability, and overall effectiveness of the predictive models.

Mean Absolute Error (MAE)

$$\mathrm{MAE} = \frac{1}{n}\sum_{i=1}^{n}|y_i - \hat{y}_i|$$

Root Mean Square Error (RMSE)

$$\mathrm{RMSE} = \sqrt{\frac{1}{n}\sum_{i=1}^{n}(y_i - \hat{y}_i)^2}$$

Coefficient of Determination ($\mathbf{R^2}$)

$$R^2 = 1 - \frac{\sum_{i=1}^{n}(y_i - \hat{y}_i)^2}{\sum_{i=1}^{n}(y_i - \bar{y})^2}$$

The $\mathbf{R^2}$ metric indicates the proportion of the variance in the dependent variable that is predictable from the independent variables, reflecting the model's explanatory power.

Each model was trained and validated using the prepared dataset, maintaining consistent training procedures and hyperparameter settings to ensure fairness in comparison. Following the training phase, key performance metrics, including Mean Absolute Error (MAE), Root Mean Square Error (RMSE), and the coefficient of determination (R^2), were calculated for each model.

In order to thoroughly assess the effectiveness of our ResUNet-O model in predicting changes in NDVI, the established assessment metrics including Root Mean Square Error (RMSE), Mean Absolute Error (MAE), and the coefficient of determination (R^2) are used. These metrics provide a quantitative evaluation of the model's precision by comparing predicted NDVI values with actual data. RMSE and MAE quantify the average size of errors in predictions, where smaller numbers indicate greater accuracy [29]. The R^2 statistic measures the degree of similarity between anticipated values and actual values, where values closer to 1 indicate higher prediction accuracy [29].

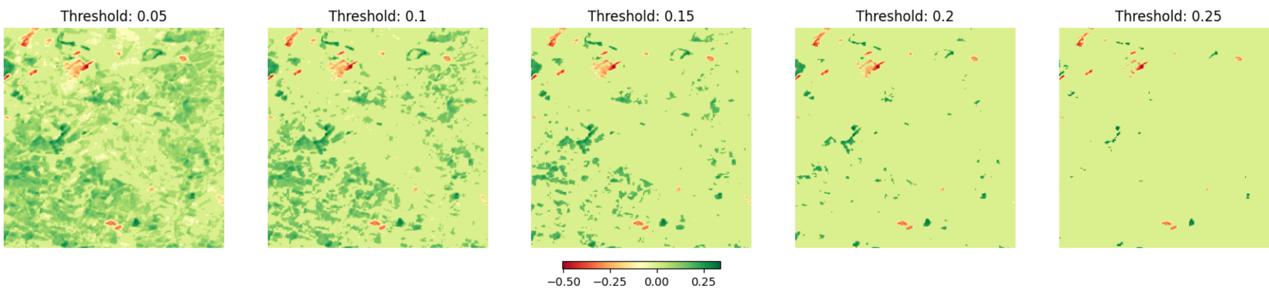

Fig. 5. Exploring different thresholds for the NDVI difference maps; lower thresholds allow for enhancement of visibility of the changes, higher thresholds retain areas with the most significant NDVI changes.

Furthermore, NDVI difference maps are created to obtain a better understanding of changes in vegetation health, in addition to the conventional measures. The difference maps, created by comparing NDVI values from 2017 and 2018, identify regions where there have been changes in the health of vegetation over a one-year period. Ground truth difference maps and predicted difference maps for the year 2018 are created. This methodology allows for visual representations and measuring the change in vegetation health, offering a clear indication of areas at risk.

Various thresholds are experimented with to visualize these changes, starting with a threshold of 0.05 to display all changes. Using higher thresholds in specific analyses yields more substantial changes in value and reduces interference, rendering them more appropriate for detailed monitoring and further processing.

3.6.5 Ablation Study

The goal of this ablation study is to assess the contribution of the various components and configurations of the overall model performance of the ResUNet-o model. Four metrics are presented: Mean Absolute Error (MAE), Root Mean Squared Error (RMSE) , R^2 (coefficient of determination), and Test Loss. Below in Table 4 are the results for each model tested.

To assess the performance and robustness of various architectures, the following models were evaluated:

- The ResUNet basic model serves as a reference point for comparing the performance of the ResUNet-O model. This model shares the same structure as the ResUNet-O model, with the only difference being the in-channels, which are set to 5 due to the absence of ontological layers in the dataset.
- A simple CNN model was used to establish a baseline performance. This model does not leverage advanced architectures like ResNet or U-Net but provides a straightforward comparison for evaluating the benefits of more complex models. No alterations have been made to the architecture, except for changing the in-channels to 8.
- The pretrained ResNet 18 model enhanced with ontological features. The ResNet architecture is well-suited for capturing complex patterns in the data due to its deep layers and residual connections. No alterations have been made to the architecture, except for changing the in-channels to 8.

The U-Net model was excluded from this comparison due to its primary focus on segmentation tasks, making it in this situation unsuitable for this particular application without adaptation.

In order to explore the impact of ontological data, the models were initially planned to be tested with and without the inclusion of these additional features. However, due to scope limitations, the models are trained and evaluated using satellite and ontological data. The purpose of this analysis was to emphasize the need of incorporating ontological data in order to enhance the accuracy and predictive abilities of the model. The ablation study has two primary objectives:

1. *Model Comparison*: To identify the most effective model architecture the model performances of the pretrained ResNet 18 are assessed including ontological data and the simple CNN model as well. This comparison will help justify the selection of the ResUNet-O model for the main analysis.
2. *Effect of Ontological Data*: To measure the impact of including ontological data on the models' predictive accuracy. By demonstrating the performance difference with and without ontological data, the study aims to validate the importance of integrating diverse data sources for more reliable predictions. This is achieved by comparing the metrics of the ResUNet-O model with the ResUNet base model.

4 Results

The results section starts by discussing the ablation study, followed by presenting the main model performance, and concluding with the presentation of visualizations.

For the assessment of model performance, the 2017 dataset was used for evaluation and consisted of 3969 samples of satellite data. The labels in the dataset corresponded to the NDVI values from the next year, 2018. The evaluation metrics include the Test Loss, Mean Absolute Error (MAE), Root Mean Square Error (RMSE), and the coefficient of determination (R^2).

4.1 Ablation Study

1. Model Comparison
The ablation study results for the model comparison, as presented in Table 4, show the comparative performance of the models in predicting NDVI values for the year 2018, using the dataset of 2017 and labels of 2018.

Model	MAE	RMSE	R^2	Test Loss	Description
ResUNet (base)	0.037352	0.045834	0.373732	0.002221	ResUNet model with satellite data
ResUNet-O	0.033658	0.043034	0.455276	0.001912	ResUNet model with satellite and ontological data
ResNet 18	0.04855	0.06107	-0.009596	0.003817	Pre-trained ResNet 18 model with satellite and ontological data
CNN	0.05679	0.07055	-0.3327	0.002966	Simple CNN model with satellite and ontological data

Table 4. Metrics based on the trained models predicting the NDVI changes for 2018.

The base ResUNet-O model, which uses satellite and ontological data, achieved the best performance with an MAE of 0.033658, RMSE of 0.043034, R^2 of 0.455276, and a test loss of 0.001912. When ontological data was excluded (ResUNet base), the performance slightly decreased, with an MAE of 0.037352 and an RMSE of 0.045834, a lower R^2 of 0.373732 and a higher test loss of 0.002221. The pre-trained ResNet 18 model, also incorporating both satellite and ontological data, performed less effectively, with an MAE of 0.04855, RMSE of 0.06107, R^2 of -0.009596, and a test loss of 0.003817, suggesting that the model had difficulties to generalize well with the given dataset. The simple CNN model demonstrated the lowest performance, with an MAE of 0.05679, RMSE of 0.07055, R^2 value of -0.3327, and a test loss of 0.002966. These results emphasize its limits in capturing the ontological features when compared to more advanced architecture such as the proposed ResUNet models.

2. Effect of Ontological Data
The metrics obtained after training are shown in Table 5 and 6. The ResUNet basic model demonstrates an average test loss of 0.0022, which is greater than the test loss of 0.0019 observed in the ResUNet-O model. It may be inferred that the ResUNet-O model has superior performance in terms of generalization on the test set. The ResUNet-O model demonstrates a slight improvement in decreasing prediction errors.

Fold	Test Loss	MAE	RMSE	R^2
1	0.001830	0.033769	0.042785	0.483536
2	0.001686	0.032213	0.041089	0.523665
3	0.001545	0.030723	0.039333	0.563515
4	0.001471	0.030394	0.038387	0.584269
5	0.004570	0.057662	0.067575	-0.288324
Average	**0.002221**	**0.037352**	**0.045834**	**0.373732**

Table 5. ResUNet base model's performance metrics after training

Fold	Test Loss	MAE	RMSE	R^2
1	0.002718	0.038572	0.052104	0.223798
2	0.001495	0.030495	0.038558	0.574916
3	0.001623	0.031867	0.040144	0.539246
4	0.001377	0.028729	0.037085	0.606790
5	0.002350	0.038628	0.048277	0.333629
Average	**0.001912**	**0.033658**	**0.043034**	**0.455276**

Table 6. ResUNet-O model's performance metrics after training

Regarding the error rates, the MAE is evaluated and it is clear from both tables that the ResUNet-O has a lower mean absolute error of 0.034 than the ResUNet base model, which has an MAE of 0.037. Therefore, also the RSME of 0.043 of the ResUNet-O models proves to be lower than the RMSE of 0.048 of the basic model. Additionally, the coefficient of determination (R^2) further emphasizes the higher performance of the ResUNet-O model. The R^2 value for the ResUNet-O is substantially greater, suggesting a better alignment of the model with the data.

4.2 Visualisations

The ResUNet-O model's ability to predict NDVI values and detect changes in vegetation health is visually demonstrated in Figure 6. This figure displays the model's predictions and maps illustrating changes in three regions of Galicia, Spain: Pontevedra, Lugo, and La Coruña.

The first column depicts the original satellite images of each area, derived from the RGB bands of the dataset. The ResUNet-O model's NDVI predictions for 2018 are displayed in the second column. These NDVI predictions are color-coded based on the NDVI values. NDVI values closer to 1 represent healthier vegetation, which is displayed by a yellow/green color. On the other hand, low values closer to -1 suggest unhealthy vegetation, which is represented by a purple/blue color. The blueish hues typically represent non-vegetation elements such as sand, water, buildings, or roadways. The third column displays the predicted change intensity maps, emphasizing regions where significant changes in

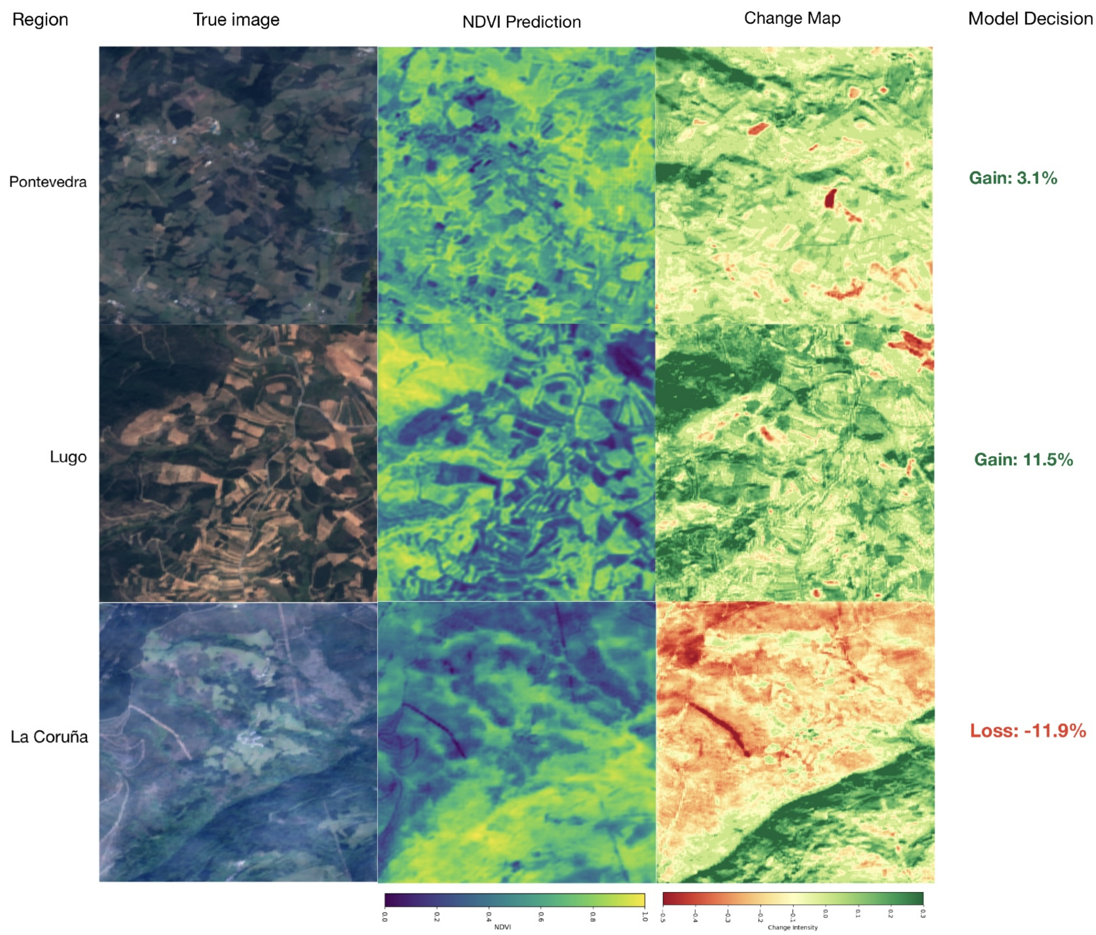

Fig. 6. True image shows the satellite image of 2018. The NDVI prediction is the prediction for 2018. The change map is the predicted change map that is calculated by the subtracting the predicted NDVI map of 2018 by the actual NDVI map of 2018.

vegetation have taken place. The color spectrum spans from red, indicating a decline in vegetation health, to green, indicating an improvement in vegetation health. The fourth column provides a quantitative measure of the total change in vegetation in each region. It summarizes the model's decision by indicating the percentage increase or decrease in vegetation health.

The change map for the Pontevedra region shows some distributed areas of vegetation growth, leading to a net NDVI increase of 3.1% between 2017 and 2018. The model in Lugo shows an even higher increase in vegetation health, with a total gain of 11.5%. The change map identifies multiple regions that have presented substantial enhancements in vegetation health, which is supported by the NDVI projections. On the other hand, La Coruña exhibits a significant decline in the health of its vegetation, resulting an overall reduction of 11.9%. The change map clearly illustrates large regions marked in red, which indicates a substantial decline in vegetation health. This image of the region La Coruña was included to illustrate the errors made by the model in the presence of cloud interference. The NDVI prediction for La Coruña reveals the presence of substantial cloud cover in the lower right area of the image.

5 Discussion

5.1 Ablation Study

By combining the UNet and ResNet models into a hybrid ResUNet architecture, it is clear that the ResUNet surpasses both the ResNet and the simple CNN model in terms of performance. Considering the findings of the performance after training, it is evident that the ResUNet-O model performs better than the basic ResUNet model. Given that the primary difference between the two models lies in the inclusion or exclusion of the ontological layers, it can be inferred that the ResUNet-O model surpasses the ResUNet base model in its performance to enhance the accuracy by including ontological data. Therefore, it can be stated that the selection of the ResUNet-O for this task is the most effective in predicting the NDVI. This provides ample evidence to proceed with further optimization of the ResUNet-O model for the purpose of making reliable and accurate NDVI predictions on forest monitoring.

Regarding the error rates, the MAE is evaluated and it is clear from both tables that the ResUNet-O has a lower mean absolute error of 0.034 than the ResUNet base model, which has an MAE of 0.037. Therefore, also the RSME of 0.043 of the ResUNet-O models proves to be lower than the RMSE of 0.046 of the basic model. This indicates that the ResUNet-O model not only provides more accurate predictions but also maintains consistency in error reduction across the dataset. A higher R^2 value indicates that a greater amount of the variability in the dependent variable can be explained by the independent variable, demonstrating the improved ability of the ResUNet-O model to understand the underlying patterns in the data. The ResUNet-O model outperforms the basic ResUNet model slightly during the training phase. Given that the single difference between these two models lies in the presence or absence of the ontological layers in the dataset, it can be inferred that there is a significant value in incorporating the ontological layers in the dataset.

Figure 7 provides a detailed comparison of vegetation changes between the years 2017 and 2018, emphasizing the effectiveness of the ResUNet-O model in predicting NDVI changes over time. This figure includes true satellite images for the years 2017 and 2018, along with the corresponding true and predicted change maps for the same period.

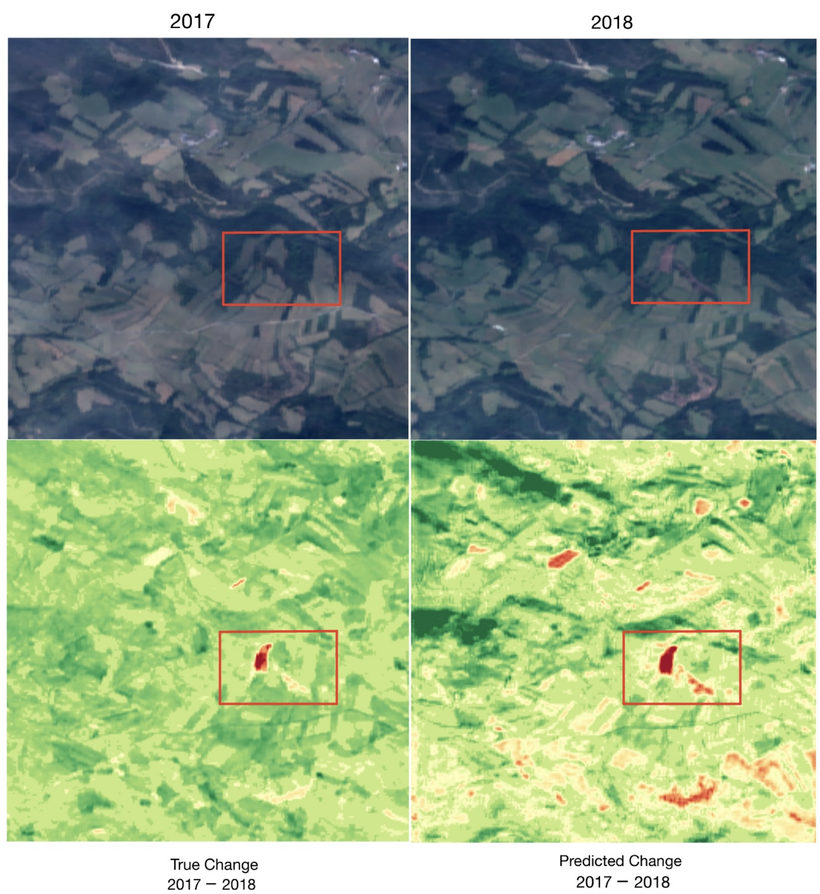

Fig. 7. The provided image displays satellite imagery from 2018 alongside NDVI predictions for the same year. The change map is generated by subtracting the predicted 2018 NDVI values from the actual 2018 NDVI values. The model decision highlights areas of gain and loss in vegetation, quantified as percentages.

The satellite images show the actual situation of 2017 and 2018. The red boxes depict the regions where deforestation has occurred during the specified time frame. The change maps display the actual changes on the left and the predicted changes in vegetation health on the right, as determined by the ResUNet-O model. The model has the capability to generate these predicted change maps in any given region, making the process of identifying deforestation-prone areas very applicable across different locations. This capability offers valuable understanding of the dynamic changes occurring in the landscape as time progresses.

5.2 Limitations

Despite the promising results of the ResUNet-O model, this study does have several limitations. The primary limitation of this research is that the research relies on the assumption that the ontological levels are not affected by time. The features provided for each band are identical for both the years 2017 and 2018. The absence of registration dates and numerous time stamps in the Cross-Forest ontology data explains this. Although, it is important to note that the species of a tree will remain the same, but it would be highly valuable to observe the changes in height and volume over time. If it were feasible to retrieve this particular dataset, it would significantly enhance the results of the model.

Additionally, the model's ability to measure changes over time is a potential limitation. By exclusively considering annual intervals, the model may overlook important seasonal fluctuations that are observed within a single year. While the process of averaging all photos from one year successfully diminished the impact of seasonal fluctuations and cloud cover on the data, it may have oversimplified the complex dynamics of vegetation health. However, this would presumably mainly apply for detailed predictions, rather than predictions on larger scale.

Furthermore, the features themselves are not evaluated. The features included in the ontological layers lack explanatory measures. It would have been beneficial to better understand the influence of these features and assess their relative significance in order to enhance the tuning of the models. Further investigation is needed to examine the correlations between changes in vegetation health and the individual development patterns of different tree species. Each species displays distinct growth patterns and varying levels of vulnerability to wildfires.

Another important issue that has been observed is that the model has a tendency to classify locations with low NDVI values, such as buildings or cloud cover, as high change of vegetation. The misclassification arises when reconstructed roads or cloud covers, which inherently possess low NDVI values, are erroneously identified as deforested regions. The absence of a segmentation procedure is the main cause of this problem, since it prevents the forest or land from being divided into sections for the purpose of assessing the risk of deforestation. This limitation emphasizes the necessity for improved segmentation between low NDVI values caused by actual vegetation loss and those arising from non-vegetative surfaces.

When examining Section 3.5.2, Figure 3 reveals a significant number of feature values within the specified area of interest. However, when examining the numbers and comparing the trees listed in the inventory with the actual quantity of trees in the area of interest, a substantial difference can be observed. The number of trees in the ontological layers is 66,352 and the actual number of trees in Galicia is 700 million. While the extent to which this gap is constraining the research is questionable, it is evident that the data is incomplete.

Lastly, one limitation is found in the collection of the Sentinel-2A imagery dataset that has a relatively lower resolution than expected. Presumably, this issue is a result of the downloaded images being of very large size. The original TIFF files, which were initially downloaded, have a dimension of 2400x2400. After undergoing processing, these files are divided into smaller images with dimensions of 256x256. This could potentially restrict the outcomes of all the models examined in this study.

To summarize, although the ResUNet model demonstrates strong potential in predicting NDVI values and monitoring vegetation health, these limitations point out a need for further improvements. To enhance the model's accuracy and generalizability, future research should focus on addressing these difficulties. This will result in more dependable measures for environmental monitoring and management.

6 Conclusion

6.1 Summary of Findings

In summary, the ResUNet-O model has demonstrated that by incorporating ontological data from the Cross-Forest ontology with the Sentinel-2A satellite images, the model was able to enhance its accuracy to predict changes in NDVI for the year 2018 in Galicia, Spain. The model demonstrated its superior performance compared to the basic ResUNet model during the training phase, as it showed lower Mean Absolute Error (MAE), Root Mean Square Error (RMSE), and higher R-squared (R^2) values. In addition, the use of change prediction maps yield vital insights for detecting substantial alterations in vegetation, hence it is able to play major roles in the identification of deforestation-prone areas.

6.2 Contributions of this Research

This research shows the importance of understanding that deforestation is a dynamic and complex problem that requires various features and functional traits to successfully capture the dynamics of deforestation. It also shows that the hybrid ResUNet-O model offers a sound solution to monitor changes in vegetation health in Galicia, Spain. It provides high-resolution predictions that can contribute to help forest monitoring systems in particular vulnerable regions as Galicia, which are prone to wildfires and other environmental stressors. This research emphasized the significance of incorporating a variety of data sources to fully capture the complex dynamics of deforestation. Even more: it provides a valuable insight that the inclusion of features as tree species, height and volume of firewood can be captured by the ResUNet model.

By demonstrating the potential of combining deep learning with ontological data, this research opens up interesting opportunities for future models to better understand and predict the complex dynamic nature of forest monitoring. All in all, this research proves the importance of recognizing that deforestation is a dynamic and complex phenomenon that requires the incorporation of various data sources in order to effectively capture and address its dynamics.

6.3 Future Work

Future research should focus on addressing the aforementioned limitations in order to enhance the outcomes of the models.

When examining the creation of the ontological layers, it is important to note that the data is incomplete. Given the understanding that incorporating ontological data is indeed improving the precision of the model, prioritizing the development of comprehensive datasets to further enhance the predicted accuracy seems to be a sound solution. This has the ability to improve forest monitoring and identify areas at risk by considering the species composition and the volume of firewood depending on the height of the trees.

While obtaining detailed data such as that found in the Cross-Forest ontology may be difficult due to its high manual labor costs, it is important to assess the extent to which the absence of such information hinders the improvement of accuracy. One approach is to generate the missing data synthetically by initially doing a tree segmentation of the area of interest to identify all trees. Subsequently, the dataset can be augmented by adding trees to areas where they are not in the dataset, but are present in the segmentation. Subsequently, the ResUNet models can be evaluated to determine if any improvements in accuracy have been made.

Another concept that this research aimed to include, but was unable to do so because of scope limitations, is to examine which tree features have a greater impact on the accuracy of the ResUNet-O model. For instance, the model can be trained by using only one feature at a time. Three models can be trained to capture three distinct features. This approach allows for the examination of the impact of species, height, and volume of firewood. An alternative approach is to generate additional data for the height and volume aspects of firewood in order to enrich the dataset with more specific information. This can be achieved by forecasting the growth of each tree individually and incorporating this information into the dataset to enhance the accuracy of predictions. This would hypothetically yield a higher accuracy when predicting for vegetation health in future years.

Further research is needed in developing models that can distinguish between low NDVI values caused by actual vegetation decline and those caused by non-vegetative surfaces like roadways. Accurate deforestation monitoring requires differentiating between various factors, which can be accomplished by using other data sources, such as maps that depict land use and land cover. Although this is not be the primary issue to address, it would be interesting to explore the outcomces of modifying the U-Net architecture in the ResUNet-O model to achieve this.

Additionally, the data's temporal resolution could be improved. Relevant studies, such as [15] and [20], have demonstrated the importance of high-resolution and temporally detailed data in environmental monitoring, suggesting that these enhancements could significantly improve model performance and utility in real-world applications. Using more precise time intervals, such as monthly increments, while considering seasonal fluctuations, could yield a more accurate examination of alterations in vegetation. Implementing this strategy could enhance the model's capacity to comprehend the dynamic characteristics of vegetation health and yield more precise forecasts.

References

1. Alzu'bi, A., Alsmadi, L.: Monitoring deforestation in jordan using deep semantic segmentation with satellite imagery. Ecological Informatics **70**, 101745 (2022)
2. Ball, J.G., Petrova, K., Coomes, D.A., Flaxman, S.: Using deep convolutional neural networks to forecast spatial patterns of amazonian deforestation. Methods in ecology and evolution **13**(11), 2622–2634 (2022)
3. Barreal, J., Jannes, G.: Spatial and temporal wildfire decomposition as a tool for assessment and planning of an efficient forest policy in galicia (spain). Forests **11**(8), 811 (2020)
4. Cohen, W.B., Yang, Z., Stehman, S.V., Schroeder, T.A., Bell, D.M., Masek, J.G., Huang, C., Meigs, G.W.: Forest disturbance across the conterminous united states from 1985–2012: The emerging dominance of forest decline. Forest Ecology and Management **360**, 242–252 (2016)
5. De Bem, P.P., de Carvalho Junior, O.A., Fontes Guimarães, R., Trancoso Gomes, R.A.: Change detection of deforestation in the brazilian amazon using landsat data and convolutional neural networks. Remote Sensing **12**(6), 901 (2020)
6. Diakogiannis, F.I., Waldner, F., Caccetta, P., Wu, C.: Resunet-a: A deep learning framework for semantic segmentation of remotely sensed data. ISPRS Journal of Photogrammetry and Remote Sensing **162**, 94–114 (2020)
7. de Diego, J., Fernández, M., Rúa, A., Kline, J.D.: Examining socioeconomic factors associated with wildfire occurrence and burned area in galicia (spain) using spatial and temporal data. Fire Ecology **19**(1), 18 (2023)
8. Fensholt, R., Langanke, T., Rasmussen, K., Reenberg, A., Prince, S.D., Tucker, C., Scholes, R.J., Le, Q.B., Bondeau, A., Eastman, R., et al.: Greenness in semi-arid areas across the globe 1981–2007—an earth observing satellite based analysis of trends and drivers. Remote sensing of environment **121**, 144–158 (2012)
9. FuenTes-sAnTos, I., Marey-Pérez, M., González-Manteiga, W.: Forest fire spatial pattern analysis in galicia (nw spain). Journal of environmental management **128**, 30–42 (2013)
10. Gao, H., Cui, K., von Gadow, K., Wang, X.: Using functional traits to improve estimates of height–diameter allometry in a temperate mixed forest. Forests **14**(8), 1604 (2023)
11. Geoghegan, J., Schneider, L., Vance, C.: Temporal dynamics and spatial scales: Modeling deforestation in the southern yucatán peninsular region. GeoJournal **61**, 353–363 (2004)

12. Giménez-García, J.M., Vega-Gorgojo, G., Ordóñez, C., Bravo, F.: Forest explorer: User-friendly navigation of iberian forestry linked open data. In: ISWC (Posters/Demos/Industry) (2023)
13. Hassan, Z., Shabbir, R., Ahmad, S.S., Malik, A.H., Aziz, N., Butt, A., Erum, S.: Dynamics of land use and land cover change (lulcc) using geospatial techniques: a case study of islamabad pakistan. SpringerPlus **5**, 1–11 (2016)
14. Hill, A., Buddenbaum, H., Mandallaz, D.: Combining canopy height and tree species map information for large-scale timber volume estimations under strong heterogeneity of auxiliary data and variable sample plot sizes. European Journal of Forest Research **137**, 489–505 (2018)
15. Huete, A.R., Didan, K., Miura, T., Rodriguez, E., Gao, X., Ferreira, L.G.: Overview of the radiometric and biophysical performance of the modis vegetation indices. Remote Sensing of Environment **83**(1-2), 195–213 (2002)
16. Huntley, B.J.: The ecological role of fire. In: Ecology of Angola: Terrestrial Biomes and Ecoregions, pp. 149–165. Springer (2023)
17. Jelas, I.M., Zulkifley, M.A., Abdullah, M.: Deforestation detection using deep learning-based semantic segmentation techniques: a systematic review. Frontiers in Forests and Global Change **7** (2024). https://doi.org/10.3389/ffgc.2024.1300060
18. Matosak, B.M., Fonseca, L.M.G., Taquary, E.C., Maretto, R.V., Bendini, H.d.N., Adami, M.: Mapping deforestation in cerrado based on hybrid deep learning architecture and medium spatial resolution satellite time series. Remote sensing **14**(1), 209 (2022)
19. Onačillová, K., Gallay, M., Paluba, D., Péliová, A., Tokarčík, O., Laubertová, D.: Combining landsat 8 and sentinel-2 data in google earth engine to derive higher resolution land surface temperature maps in urban environment. Remote Sensing **14**(16), 4076 (2022)
20. Pettorelli, N., Vik, J.O., Mysterud, A., Gaillard, J.M., Tucker, C.J., Stenseth, N.C.: Using the satellite-derived ndvi to assess ecological responses to environmental change. Trends in ecology & evolution **20**(9), 503–510 (2005)
21. Ronneberger, O., Fischer, P., Brox, T.: U-net: Convolutional networks for biomedical image segmentation. In: Medical image computing and computer-assisted intervention–MICCAI 2015: 18th international conference, Munich, Germany, October 5-9, 2015, proceedings, part III 18. pp. 234–241. Springer (2015)
22. Rosa, I.M., Purves, D., Souza Jr, C., Ewers, R.M.: Predictive modelling of contagious deforestation in the brazilian amazon. PloS one **8**(10), e77231 (2013)
23. Roy, P.S., Ramachandran, R.M., Paul, O., Thakur, P.K., Ravan, S., Behera, M.D., Sarangi, C., Kanawade, V.P.: Anthropogenic land use and land cover changes—a review on its environmental consequences and climate change. Journal of the Indian Society of Remote Sensing **50**(8), 1615–1640 (2022)
24. Sboui, T., Saidi, S., Lakti, A.: A machine-learning-based approach to predict deforestation related to oil palm: Conceptual framework and experimental evaluation. Applied Sciences **13**(3), 1772 (2023)
25. Schafer, J.L., Breslow, B.P., Hohmann, M.G., Hoffmann, W.A.: Relative bark thickness is correlated with tree species distributions along a fire frequency gradient. Fire Ecology **11**, 74–87 (2015)
26. Stevens-Rumann, C.S., Sieg, C.H., Hunter, M.E.: Ten years after wildfires: How does varying tree mortality impact fire hazard and forest resiliency? Forest Ecology and Management **267**, 199–208 (2012)

27. Sun, Y., Lao, D., Ruan, Y., Huang, C., Xin, Q.: A deep learning-based approach to predict large-scale dynamics of normalized difference vegetation index for the monitoring of vegetation activities and stresses using meteorological data. Sustainability **15**(8), 6632 (2023)
28. Tucker, C.J.: Red and photographic infrared linear combinations for monitoring vegetation. Remote Sensing of Environment **8**(2), 127–150 (1979)
29. Ullah, B., Fawad, M., Khan, A.U., Mohamand, S.K., Khan, M., Iqbal, M.J., Khan, J.: Futuristic streamflow prediction based on cmip6 scenarios using machine learning models. Water Resources Management **37**(15), 6089–6106 (2023)
30. Zhang, X., Jin, X.: Vegetation dynamics and responses to climate change and anthropogenic activities in the three-river headwaters region, china. Ecological Indicators **131**, 108223 (2021)
31. Zhu, X.X., Tuia, D., Mou, L., Xia, G.S., Zhang, L., Xu, F., Fraundorfer, F.: Deep learning in remote sensing: A comprehensive review and list of resources. IEEE geoscience and remote sensing magazine **5**(4), 8–36 (2017)

7 Appendix

https://github.com/christyesmee/Thesis

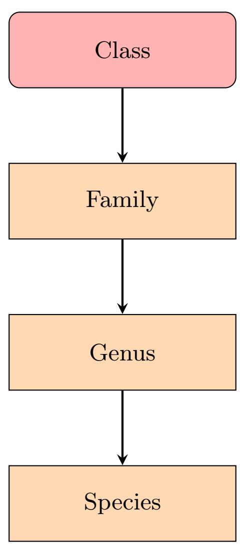

Fig. 9. Hierarchy of tree species in the ontology.

Fig. 8. Deforestation between the years 2017 and 2018.

Table 7. Samples with Missing Values for Firewood

Index	Height	Firewood	Xcoord	Ycoord	Species Number
848	11.0	0.000000	-8.164131	42.312202	43.0
849	12.0	0.000000	-8.164163	42.312177	41.0
850	8.5	0.000000	-8.164129	42.312212	41.0

Table 8. Extracted and Cleaned Ontology Data

Index	Height	Firewood	Xcoord	Ycoord	Species Number
0	17.0	57.230344	-7.700597	42.434027	41.0
3	23.0	84.983778	-7.931573	42.436231	26.0
40	17.0	11.489096	-7.855251	41.949272	273.0
411	11.5	0.000000	-8.565462	42.170395	61.0
826	7.5	9.718874	-8.039768	42.509313	657.0
863	13.5	44.657181	-7.728068	42.281247	43.0

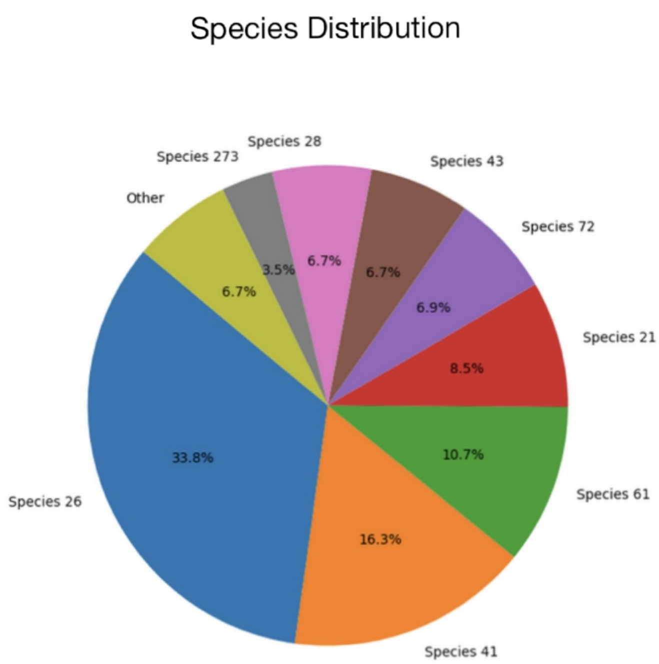

Fig. 10. Species distribution of the cleaned ontological data, highlighting the top 8 species with the highest occurrence percentages in the dataset, indicating their prevalence in the logged tree data for Galicia.